

**Chalmers Publication Library**



## Copyright Notice

This paper was published in *Optics Express* and is made available as an electronic reprint with the permission of OSA. The paper can be found at the following URL on the OSA website: <http://dx.doi.org/10.1364/OE.20.007544>. Systematic or multiple reproduction or distribution to multiple locations via electronic or other means is prohibited and is subject to penalties under law.

*(Article begins on next page)*

# Transmission of PM-QPSK and PS-QPSK with different fiber span lengths

Martin Sjödin,<sup>1,\*</sup> Ben J. Puttnam,<sup>2</sup> Pontus Johannisson,<sup>1</sup> Satoshi Shinada,<sup>2</sup> Naoya Wada,<sup>2</sup> Peter A. Andrekson,<sup>1</sup> and Magnus Karlsson<sup>1</sup>

<sup>1</sup>Department of Microtechnology and Nanoscience, Chalmers University of Technology, Kemivägen 9, SE-41296 Göteborg, Sweden.

<sup>2</sup>Photonics Networks Group, National Institute of Information and Communications Technology, 4-2-1 Nukui-Kita-Machi, Koganei, Tokyo, 184-8795, Japan

\*[martin.sjodin@chalmers.se](mailto:martin.sjodin@chalmers.se)

**Abstract:** We perform experimental and numerical investigations of the transmission reach of polarization-switched QPSK (PS-QPSK) and polarization-multiplexed QPSK (PM-QPSK) for three different fiber span lengths: 83, 111 and 136 km. In the experimental comparison we investigate the performance of PS-QPSK at 20 Gbaud and PM-QPSK at the same bit rate (60 Gbit/s) and at the same symbol rate, both the single channel case and a WDM system with 9 channels on a 50 GHz grid. We show that PS-QPSK gives significant benefits in transmission reach for all span lengths. Compared to PM-QPSK, use of PS-QPSK increases the reach with more than 41% for the same symbol rate and 21% for the same bit rate. In the numerical simulations we use the same data rates as in the experiment. The simulation results agree well with the experimental findings, but the transmission reach is longer due to the absence of various non-ideal effects and higher back-to-back sensitivity. Apart from using data coded in the absolute phase in the simulations, we also investigate differentially coded PS-QPSK for the first time and compare with PM-QPSK with differential coding. The power efficiency advantage of PS-QPSK then increases with approximately 0.3 dB at a bit error rate of  $10^{-3}$ , resulting in a further relative transmission reach improvement over PM-QPSK. Both the experimental and the numerical results indicate that PS-QPSK has slightly higher tolerance to inter-channel nonlinear crosstalk than PM-QPSK.

©2012 Optical Society of America

**OCIS codes:** (060.0060) Fiber optics and optical communications; (060.1660) Coherent communications.

---

## References and links

1. M. Karlsson and E. Agrell, "Which is the most power-efficient modulation format in optical links?" *Opt. Express* **17**(13), 10814–10819 (2009).
2. E. Agrell and M. Karlsson, "Power-efficient modulation formats in coherent transmission systems," *J. Lightwave Technol.* **27**(22), 5115–5126 (2009).
3. M. Karlsson and E. Agrell, "Generalized pulse-position modulation for optical power-efficient communication," *Proc. of ECOC 2011*, Tu.6.B.6 (2011).
4. P. Poggiolini, G. Bosco, A. Carena, V. Curri, and F. Forghieri, "Performance evaluation of coherent WDM PS-QPSK (HEXA) accounting for non-linear fiber propagation effects," *Opt. Express* **18**(11), 11360–11371 (2010).
5. P. Serena, A. Vannucci, and A. Bononi, "The performance of polarization-switched QPSK (PS-QPSK) in dispersion managed WDM transmissions," *Proc. of ECOC 2010*, Th.10.E.2 (2010).
6. M. Sjödin, P. Johannisson, H. Wymeersch, P. A. Andrekson, and M. Karlsson, "Comparison of polarization-switched QPSK and polarization-multiplexed QPSK at 30 Gbit/s," *Opt. Express* **19**(8), 7839–7846 (2011).
7. J. K. Fischer, L. Molle, M. Nölle, D.-D. Grob, and C. Schubert, "Experimental investigation of 28-GBd polarization-switched quadrature phase-shift keying signals" *Proc. of ECOC 2011*, Mo.2.B.1 (2011).
8. D. Lavery, C. Behrens, S. Makovejs, D. S. Millar, R. I. Killey, S. J. Savory, and P. Bayvel, "Long-haul transmission of PS-QPSK at 100 Gb/s using digital backpropagation," *IEEE Photon. Technol. Lett.* **24**(3), 176–178 (2012).
9. D. S. Millar, D. Lavery, S. Makovejs, C. Behrens, B. C. Thomsen, P. Bayvel, and S. J. Savory, "Generation and long-haul transmission of polarization-switched QPSK at 42.9 Gb/s," *Opt. Express* **19**(10), 9296–9302 (2011).

10. L. E. Nelson, X. Zhou, N. Mac Suibhne, A. D. Ellis, and P. Magill, "Experimental comparison of coherent polarization-switched QPSK to polarization-multiplexed QPSK for  $10 \times 100$  km WDM transmission," *Opt. Express* **19**(11), 10849–10856 (2011).
11. J. Renaudier, O. Bertran-Pardo, H. Mardoyan, M. Salsi, P. Tran, E. Dutisseuil, G. Charlet, and S. Bigo, "Experimental investigation of 28Gbaud polarization switched- and polarization division multiplexed-QPSK in WDM long-haul transmission system," *Proc. of ECOC 2011*, Mo.2.B.3 (2011).
12. M. Nölle, J. K. Fischer, L. Molle, C. Schmidt-Langhorst, D. Peckham, and C. Schubert, "Comparison of  $8 \times 112$  Gb/s PS-QPSK and PDM-QPSK signals over transoceanic distances," *Opt. Express* **19**(24), 24370–24375 (2011).
13. A. J. Viterbi and A. M. Viterbi, "Nonlinear estimation of PSK-modulated carrier phase with application to burst digital transmission," *IEEE Trans. Inf. Theory* **29**(4), 543–551 (1983).
14. P. Johannisson, M. Sjödin, M. Karlsson, H. Wymeersch, E. Agrell, and P. A. Andrekson, "Modified constant modulus algorithm for polarization-switched QPSK," *Opt. Express* **19**(8), 7734–7741 (2011).
15. D. Wang and C. R. Menyuk, "Polarization evolution due to the Kerr nonlinearity and chromatic dispersion," *J. Lightwave Technol.* **17**(12), 2520–2529 (1999).

## 1. Introduction

Coherent transmission based on polarization-multiplexed quadrature phase-shift keying (PM-QPSK) has enjoyed a lot of success in recent years due to its relative ease of implementation and good spectral efficiency. In addition, PM-QPSK has relatively high power efficiency and is thus suitable for long-haul transmission. However, several other power-efficient modulation formats also exist and may be of interest for implementation in future fiber optic communication systems. For example, by taking a particular subset of the PM-QPSK symbol alphabet, a format conveniently described as QPSK transmitted in one selected polarization-state per symbol duration, can be created. This format is known as polarization-switched QPSK (PS-QPSK) [1, 2]. Together with 2-pulse-position QPSK, PS-QPSK is the most power efficient modulation format in signal spaces with up to four dimensions [1–3]. It has similar implementation complexity as PM-QPSK and has attracted a lot of attention recently. The transmission performance of PS-QPSK was first investigated with numerical simulations, showing that it is a direct competitor to PM-QPSK at the same bit rate [4, 5]. Furthermore, it has been suggested that PS-QPSK is useful as a fallback option to keep a degraded PM-QPSK-based link in operation by switching modulation format with maintained symbol rate, at the expense of a 25% bit rate reduction [4]. These simulation studies also indicated higher tolerance for PS-QPSK to nonlinear crosstalk between WDM channels.

The increased sensitivity and robustness to nonlinearities are attractive features as they allow for extended transmission reach compared to PM-QPSK, as has been shown in several experiments: In [6], PS-QPSK was generated for the first time by using a novel transmitter, and the sensitivity advantage over PM-QPSK was confirmed. In other single channel experiments, Fischer *et al.* presented a comparison of PS- and PM-QPSK in an ultra large area fiber link over transoceanic distances [7], and demonstrated significant improvement in reach with PS-QPSK, and Lavery *et al.* demonstrated 20% improvement in transmission distance (from 4650 km to 5620 km at a BER of  $3.0 \cdot 10^{-3}$ ) for PS-QPSK at 112 Gbit/s by using digital back-propagation after coherent detection [8].

Experimental WDM results comparing the two formats have also been presented. In [9], 30% longer transmission reach was achieved for PS-QPSK for a BER of  $3.8 \cdot 10^{-3}$  in the receiver in a system with seven 40 Gbit/s 50 GHz-spaced channels (0.8 bit/s/Hz spectral efficiency). In [10], PS-QPSK at 40.5 Gbit/s tolerated 1.6 dB higher launch power per channel to achieve a BER of  $10^{-3}$  in the receiver in  $10 \times 100$  km 50 GHz-spaced WDM transmission. Renaudier *et al.* reported a comparison between the formats at 28 Gbaud, in which PS-QPSK achieved 3 dB higher Q factor than PM-QPSK after transmission in a 4800 km link with hybrid Raman-Erbium optical repeaters [11], and Nölle *et al.* recently demonstrated 10% increase in transmission reach at a BER of  $3.8 \cdot 10^{-3}$  in the receiver when comparing PS- and PM-QPSK in a WDM system with eight 50 GHz-spaced channels at 112 Gbit/s [12].

As PS-QPSK has high sensitivity and robustness to nonlinear effects, it may be possible to use longer fiber spans in a link and at the same time reduce the number of erbium-doped amplifiers (EDFAs), which is attractive from a cost perspective. However, a comparison of

the performance of PS-QPSK and PM-QPSK for different fiber span lengths has not yet been presented. Hence, we here report the results of an experimental comparison of 20 Gbaud PS-QPSK with PM-QPSK at the same bit rate (60 Gbit/s) and at the same symbol rate. We use a wavelength division multiplexing (WDM) system with nine channels on a 50 GHz frequency grid and a single-span recirculating loop with three different fiber span lengths of 83, 111, and 136 km. We find a significant increase in reach with PS-QPSK for all span lengths, even when comparing with PM-QPSK at the same bit rate.

Numerical simulations were performed after the experiment to support the results and investigate the impact of hardware limitations, in particular the use of a single-span loop. We found that the transmission reach in the experiment has better agreement with the simulation results for longer span lengths, which is most likely due to a smaller impact from loop-specific impairments such as filter gain ripples and polarization-dependent loss (PDL). Both the experimental and the numerical results confirm the higher robustness of PS-QPSK to inter-channel nonlinearities, but the difference is small when the optimal fiber span launch power is used.

A new scheme for differential coding of PS-QPSK is also investigated in the simulations and a comparison is made with PM-QPSK with differential coding. We show that the advantage of PS-QPSK in terms of sensitivity and transmission reach is further increased when differential coding is used.

## 2. Experimental setup

Figure 1(a) shows the PS-QPSK transmitter together with simulated constellation diagrams of PS-QPSK in the two orthogonal polarization states  $x$  and  $y$ . An IQ-modulator (IQM) driven by two binary signals generated a QPSK signal in a single polarization. The signal was split 50/50 and Mach-Zehnder modulators (MZM) followed by a polarization beam-combiner (PBC) provided polarization switching. The MZMs were driven by data and data inverse of a third binary signal and as a result only one MZM was transmitting during each symbol period. PM-QPSK was generated as shown in Fig. 1(b), by splitting and recombining a QPSK signal with a relative time delay  $\Delta T$  of about 4.5 ns, with the exact value being an integer number of symbol slots. Similarly to Fig. 1(a), the constellation diagrams of PM-QPSK in the  $x$ - and the  $y$ -polarization are shown in the Fig. insets. All data streams were  $2^{15}-1$  pseudo-random bit sequences (PRBS) and the maximum symbol rate was restricted to 20 Gbaud due to hardware limitations. Gray-coded bit-to-symbol mapping was used for the QPSK data.

Figure 1(c) shows the method used to decorrelate the data of neighboring WDM channels. The even and the odd channels were separated with a 50/100 GHz interleaver filter and recombined with a relative time delay  $\Delta T_1$  of 9 ns. Since most of the signal power was within a bandwidth smaller than the channel spacing this scheme did not result in any noticeable performance degradation for the range of BER values investigated in this work.

The recirculating loop is shown in Fig. 1(d), and is similar to the one used in [8, 9]. A gain-flattened EDFA and a variable attenuator were used to set the launch power into a span of standard single-mode fiber (SSMF). The span losses were 17.0, 22.5, and 27.9 dB for span lengths of 83, 111, and 136 km, respectively. The loss of the other loop components was 13 dB in total. A second gain-flattened EDFA boosted the power after the fiber and a gain flattening filter was used to equalize the power of the WDM channels and ensure less than  $\pm 1.0$  dB power variation, relative to the center channel, in the receiver. The number of loop circulations was controlled with acousto-optic modulators (AOM) driven by complementary control pulses. The Doppler frequency shift of the loop AOM was compensated for by an

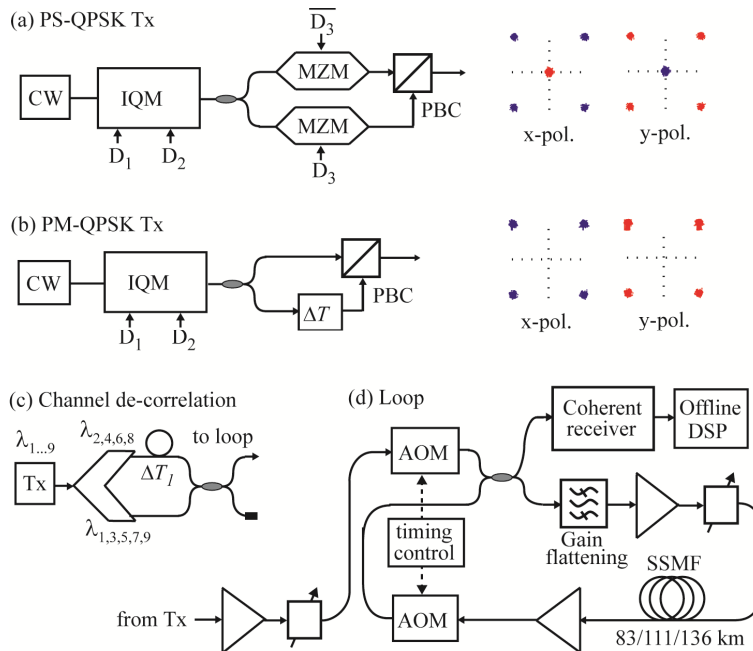


Fig. 1. The experimental setup. (a) PM-QPSK transmitter. (b) PS-QPSK transmitter. (c) Decorrelation of odd and even WDM channels. (d) The transmission loop used for long-haul transmission.

additional AOM in the loop (not shown in Fig. 1). The loop noise figure, taking the loss between the amplifiers into account, was 5.5 dB.

The motivation to use a single fiber span is that it makes it easy to change between different span lengths. We used no polarization controllers (nor any synchronous scrambling) inside the loop, but allowed for arbitrary polarization drifts. Since we used polarization multiplexed data, we believe that the performance will not be significantly affected by the absence of a scrambler, but the emulation of a real system and its polarization statistics will not be as good. A potential problem may be PDL, which was measured to be below 0.1 dB in the loop (limited by measurement capabilities), but which may obviously be significantly higher after many roundtrips. However in the measurements we never saw any significant performance difference between the two polarizations, which indicates that the effects of PDL were of limited influence. Even though PDL may also cause depolarization, which increases the BER in both polarization tributaries, significant impact from this effect should during the course of the experiment have caused a noticeable performance difference between the x- and the y-polarized signals. Another well-known issue with recirculating loop experiments is the impact from ripples of the gain-flattening filters or any other filters present. This effect can partly be compensated for by the equalizer after coherent detection, but it may give a performance penalty that increases with the number of round-trips.

We used a coherent receiver with a polarization-diversity optical 90° hybrid to detect the center channel and measure the bit error rate. The optical front-end and a block diagram of the digital signal processing (DSP) are shown in Fig. 2. The four outputs from the optical hybrid were sampled synchronously and digitized at 50 GSamples/s by ADCs with 16 GHz analog bandwidth and the two complex photocurrents  $i_x$  and  $i_y$  (received in the orthogonal polarization states x and y) were processed offline. After downsampling to two samples per symbol, static compensation for receiver front-end imperfections was performed. This was followed by low-pass filtering (5th order Bessel filter) with 3-dB bandwidth of 0.75 times the

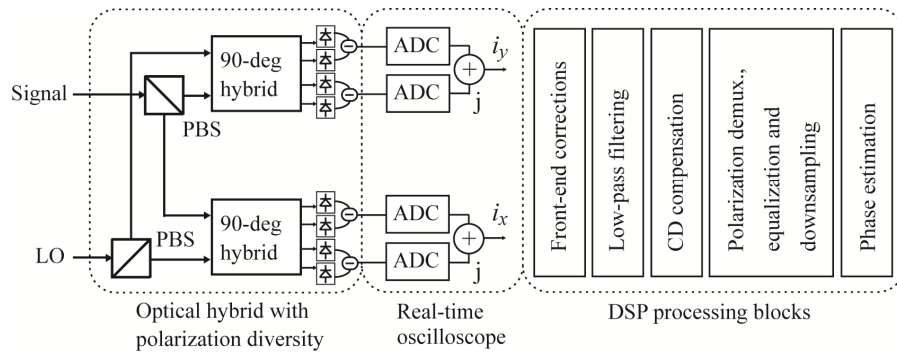


Fig. 2. The coherent receiver used to detect the signal, and the DSP blocks.

symbol rate for noise suppression, chromatic dispersion compensation in the frequency domain, polarization demultiplexing, equalization, downsampling to one sample per symbol and finally compensation for random phase fluctuations due to laser phase noise. The Viterbi-Viterbi algorithm was used for phase estimation [13]. For PM-QPSK, the phase was estimated separately for  $i_x$  and  $i_y$ , while for PS-QPSK we performed joint phase estimation by comparing the amplitudes of  $i_x$  and  $i_y$  for each symbol and choosing the sample with the largest power for phase estimation. Before the phase estimation for PS-QPSK, the phase offset between  $i_x$  and  $i_y$ , was compensated by applying the Viterbi-Viterbi algorithm on a block of data (with a few hundred symbols) from each tributary. The linewidth of the center channel laser was about 100 kHz and, to save hardware, the same laser was also used as local oscillator (LO) in the receiver. The phases of the signal and of the LO were decorrelated due to the long transmission distances. Due to the narrow laser linewidth, no cycle slips were encountered during the phase estimation in our experiment.

The main difference in the DSP of PS-QPSK and PM-QPSK is the polarization demultiplexing, since CMA does not work for PS-QPSK. For this format we instead used the algorithm described in [14], which has similar convergence and polarization tracking performance as CMA. For both formats, we measured the BER of the center channel as a function of the transmission distance and the launch power per channel into the SSMF span. To overcome the polarization ambiguity in the receiver after transmission, a sequence of the known PRBS pattern was identified.

### 3. Numerical simulations

We carried out numerical simulations covering every case studied in the experiment. The motivation for the simulations is not to exactly emulate the experimental setup in all aspects, but to see if the experimental results are reasonable and if the conclusions would be different with a setup in which penalties from e.g. thermal noise, ADC resolution, and filter gain ripples are absent.

As a model for light propagation in an optical fiber, we used the Manakov model together with attenuation [15]. The Manakov equation describes propagation in a fiber with rapidly and randomly varying birefringence, which is the case for most sufficiently long transmission fibers. We used the following parameter values in the simulations: Dispersion coefficient  $D = 17$  ps/nm/km, dispersion slope  $S = 0.07$  ps/nm<sup>2</sup>/km, nonlinear coefficient  $\gamma = 1.2$ /W/km and attenuation constant  $\alpha = 0.205$  dB/km. The fiber link consisted of a repeated number of identical sections with an EDFA followed by a span of SSMF. The same span lengths as in the experiment (83, 111 and 136 km) were used. The EDFA noise figure was set to 5.5 dB and ASE noise was added at each amplifier stage. As in the experiment, the BER was calculated as a function of the fiber span launch power per channel and the transmission distance. Polarization-mode dispersion and laser phase noise were neglected in the simulations, as their impact on the experimental results was small. All channels were launched co-polarized, as it

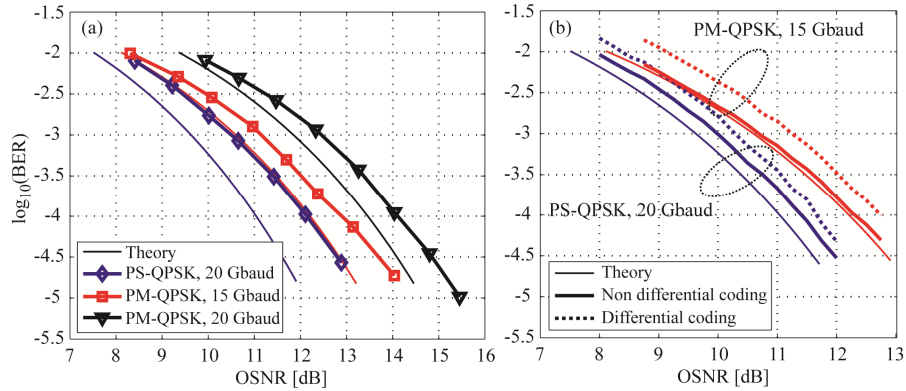


Fig. 3. (a) The experimentally measured back-to-back BER together with the theory. (b) Simulation data results for non-differential and differential coding of data. Theoretical results for non-differential coding are included for comparison.

has been shown that the launch polarization alignment has negligible practical impact [4, 5]. For PS- and PM-QPSK modulation we used random binary data sequences with  $2^{15}$  symbols and the same transmitter types as in the experiment. The electrical driving signals were bandwidth-limited by 5th order Bessel filters with bandwidths of 0.75 times the symbol rate. The 50/100 GHz interleaver was modeled as a 2nd order super-Gaussian filter with 45 GHz 3-dB bandwidth, giving good agreement with the measured frequency response of the device used in the experiment. The loop filter was a 4th order super-Gaussian filter with bandwidth depending on the number of channels. The same DSP as in the experiment was used in the receiver, with the exception of the laser phase noise tracking. For every case, simulations were repeated until at least 500 bit errors had been counted at a BER of  $10^{-3}$ .

We investigated both non-differential and differential coding. The latter case has so far not yet been studied for PS-QPSK, but is relevant since differential modulation has the benefit of avoiding error bursts due to phase cycle slips. With differentially coded PS-QPSK, two bits are coded in the transitions between the quadrants in the complex plane and the third bit in the choice of polarization state. It is also possible to encode the bit determining the launch polarization differentially, but that would give a higher BER, as every symbol error caused by an incorrect decision on the launch polarization state would give two bit errors instead of one.

In the decoding of PS-QPSK with differential coding, a decision is first made on the launch polarization state of the QPSK symbol, and the differential transition is decided by comparing with the preceding symbol. To avoid error bursts due to phase cycle slips, which is the main motivation to use differential coding, joint phase estimation is required for PS-QPSK (but not for PM-QPSK) for the signals from the different polarization tributaries. For both types of coding, Gray-mapping was used for the QPSK symbols for both PS- and PM-QPSK.

#### 4. Experimental and numerical results and discussion

In this section we present and discuss the experimental and numerical results for PS-QPSK and PM-QPSK. When we compare the formats in terms of transmission reach, sensitivity, etc., we do so at a BER in the receiver of  $10^{-3}$ .

The back-to-back BER was measured and simulated for both formats and the results are shown in Fig. 3(a) and Fig. 3(b), respectively, together with the theoretical limits. For PM-QPSK the experimental implementation penalty compared to the theory was 0.6 dB at both 15 and 20 Gbaud, while it was 0.9 dB for PS-QPSK. We attribute the larger penalty for PS-QPSK to the additional transmitter hardware needed for polarization switching. However, even with the additional penalty, the advantage for PS-QPSK over PM-QPSK is still 0.7 dB and 1.9 dB when comparing the formats at the same bit rate and the same symbol rate, respectively. The linear WDM crosstalk and the impact of the interleaver filter used to

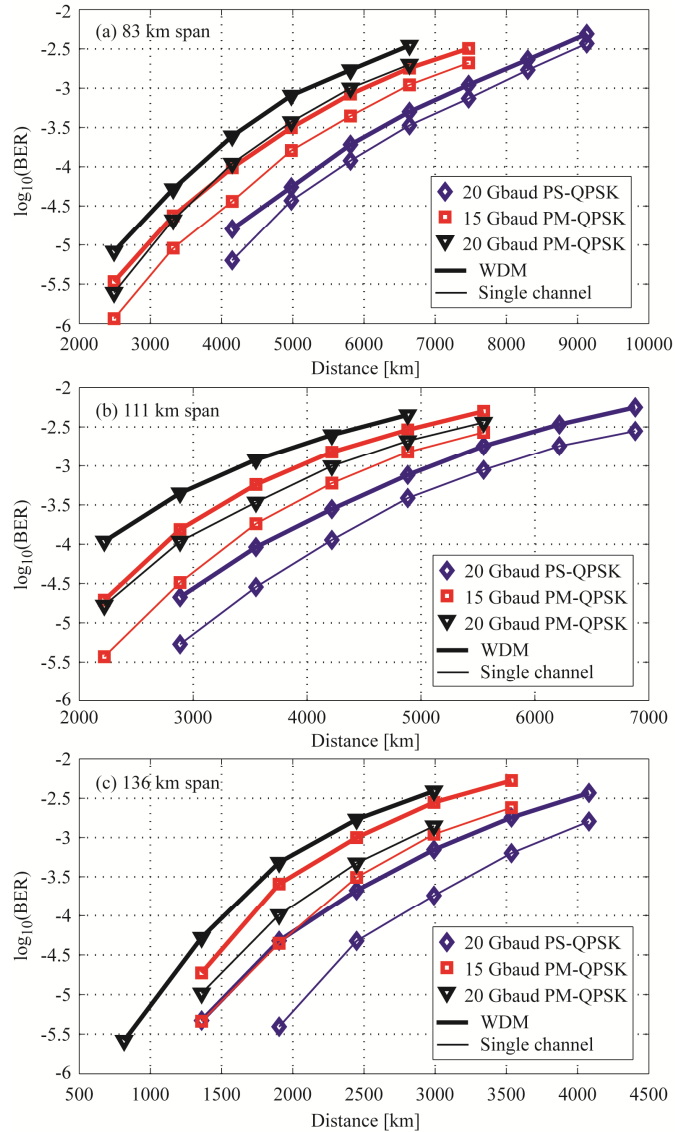


Fig. 4. Experimentally measured BER at the receiver as a function of the transmission distance for the different span lengths. (a) 83 km. (b) 111 km. (c) 136 km.

decorrelate the neighboring channels were both negligible for the investigated BER values.

The simulation results, shown in Fig. 3(b), are closer to the theory. This is expected due to the absence of driving signal reflections, thermal noise and other detrimental effects absent in the simulations. As in the experiment, the implementation penalty is slightly larger for PS-QPSK (0.4 dB compared to 0.1 dB for PM-QPSK) due to the limited bandwidth of the amplitude modulation used for polarization switching. Even though the equalizer after coherent detection can compensate for bandwidth limitations, perfect compensation of this effect cannot be expected due to noise enhancement. It is interesting to note that with differential coding PS-QPSK has an additional advantage over PM-QPSK in terms of required OSNR of about 0.3 dB at the target BER. The explanation for this is that two out of three bits are differentially coded for PS-QPSK, compared to all four bits for PM-QPSK. As a result, the differential coding penalty is larger for PM-QPSK, which for differential coding gets two



bit errors for every symbol error at reasonable OSNR, resulting in 0.55 dB penalty at a BER of  $10^{-3}$ . The penalty from linear WDM crosstalk and the interleaver filter was negligible for all simulated cases.

Figures 4(a)-(c) show the BER in the receiver as a function of the transmission distance for the three span lengths. The optimal fiber span launch power to achieve the target BER of  $10^{-3}$  was used to obtain these results. For a span length of 83 km, there is a quite small difference between the WDM reach and the single channel reach. For the longer spans, the optimal launch power is higher which increases the influence of nonlinear WDM crosstalk. Subsequently, the difference between the WDM reach and the single channel reach is larger. This is most easily seen in Fig. 4(c), which shows the reach for the 136 km span.

Figures 5(a)-(b) show how the optimal launch power into each SSMF span depends on the fiber span length in the experiment and the simulations, respectively. In the experiment, the optimal launch power is 0.5-1.5 dB smaller in the WDM case than for single channel transmission, which is explained by the presence of nonlinear crosstalk between the WDM channels. In the simulations the difference is in the range 0.5-1.0 dB. The observed increase in launch power as a function of the span length is due to the higher attenuation losses for the longer spans. The optimal launch power is slightly lower in the simulations, which is most likely due to the limited accuracy of simulation parameters such as the loop noise figure or the nonlinear coefficient. Still, the general trend is very similar in the experiment and the simulations, with one exception: For the 136 km span and single channel PS-QPSK transmission, the measured optimal launch power, shown in Fig. 4(a), is 0.5-1.0 dB higher than what may be expected from looking at the general trend in the curves from the other measurements and the simulations. However, the reach of the signal does not change much with a deviation of  $\pm 1$  dB from the optimal power, and for this reason we do not think this has an impact on the comparison between PS- and PM-QPSK.

Figure 6 shows the increase in reach when using PS-QPSK instead of PM-QPSK as a function of the fiber span length. The experimental results are shown in Fig. 6(a). At the same symbol rate of 20 Gbaud, the reach in the WDM case can be extended more than 41% for all span lengths if PS-QPSK is used, while the increase with a bit rate of 60 Gbit/s for both formats is more than 21%. Figure 6(b) shows the simulation results with non-differential coding. Comparing the formats at the same symbol rate, more than 47% increase in WDM reach can be obtained when using PS-QPSK instead of PM-QPSK at 20 Gbaud. At the same bit rate more than 30% increase is possible. The advantage when using PS-QPSK is larger in the simulations, in particular for the shortest span length. The main reason is probably that the impact from filter gain ripple, PDL and other sources of degradation affect PS-QPSK more because the number of loop circulations is larger for this format. Even though the impact from such effects is small, it is not completely negligible and could partly explain the difference between the experimental and the numerical results.

Figure 6(c) shows the simulation results with differential coding of the data. The difference between the formats increases slightly due to the increased relative difference in required OSNR. At the same symbol rate, PS-QPSK gives more than 52% WDM reach increase for all span lengths, and at 60 Gbit/s the increase is more than 42%. On average, PS-QPSK with differential coding achieves 93% of the reach for non-differential coding both for the single channel case and for the WDM case. The corresponding number for PM-QPSK is 88%. The trend is that PS-QPSK has slightly higher tolerance than PM-QPSK to nonlinear WDM crosstalk, as the difference between the formats generally is larger in the WDM case in both the experiment and in the simulations. Significant performance advantage for PS-QPSK in the nonlinear regime has been reported previously in [4, 5]. However, in this work we compare the formats at the optimal launch power to achieve a BER of  $10^{-3}$ , and at these power levels the impact from inter-channel nonlinearities appear to be similar.

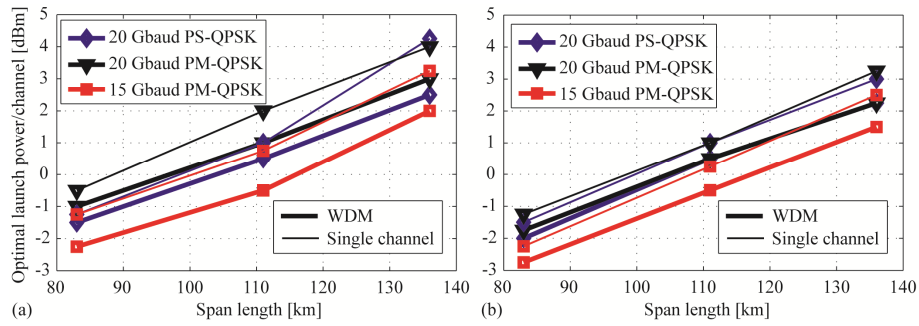


Fig. 5. Optimal launch power as a function of the span length for PS- and PM-QPSK. (a) In the experiment. (b) In the simulations.

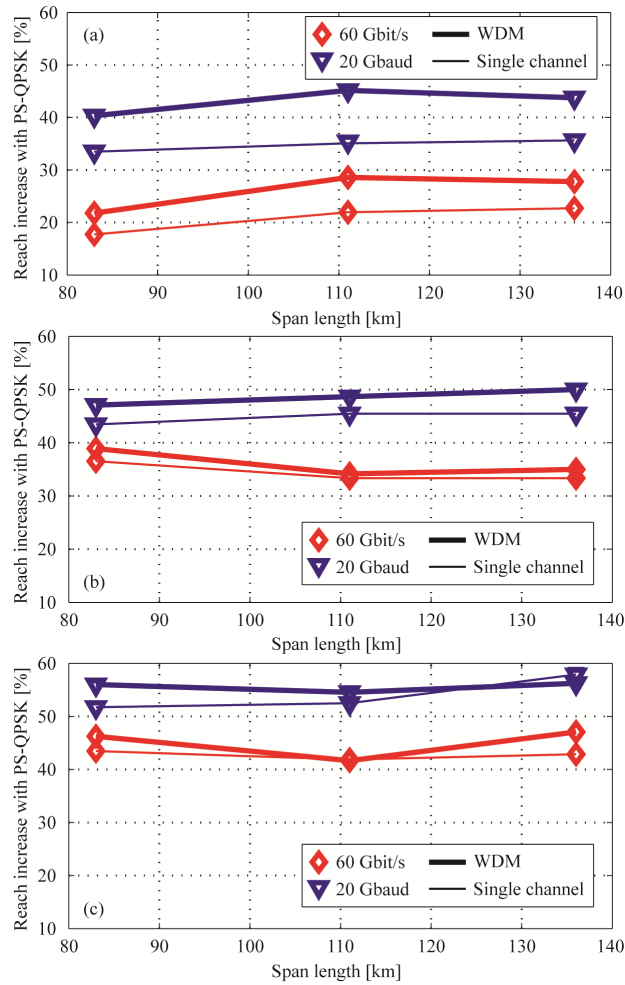


Fig. 6. Reach increase when using PS-QPSK instead of PM-QPSK as a function of the fiber span length. (a) Experimental results with non-differential coding. (b) Simulations with non-differential coding. (c) Simulations with differential coding.

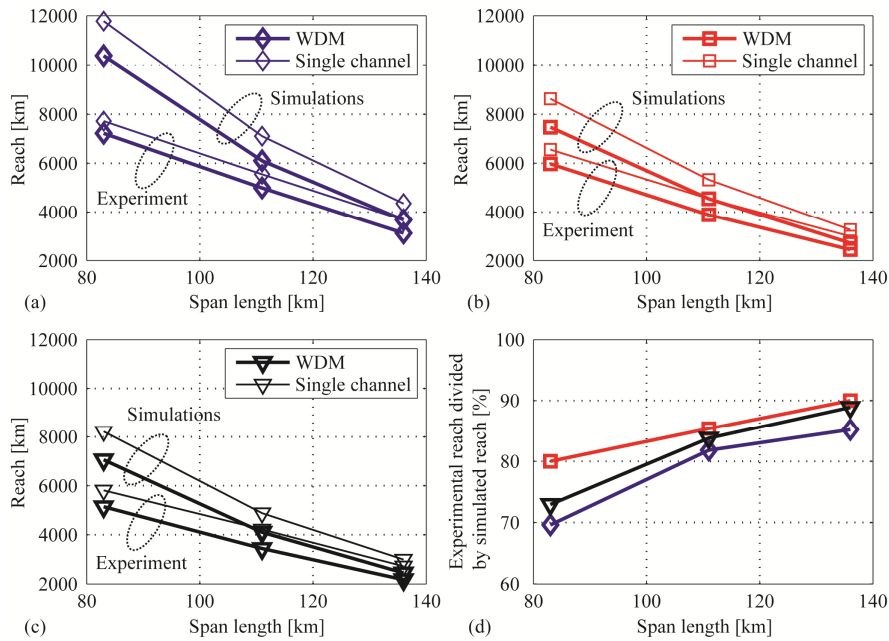


Fig. 7. Comparison of the transmission reach in the experiment with the transmission reach in the simulations for (a) PS-QPSK at 20 Gbaud, (b) PM-QPSK at the same bit rate (60 Gbit/s), and (c) PM-QPSK at 20 Gbaud. (d) The WDM reach in the experiment divided by the WDM reach in the simulations for each case. The same legend as in (a)-(c) applies.

Figures 7(a)-(c) show, for non-differential coding, comparisons of the reach in the experiment with the reach in the simulations. Figure 7(d) shows, for the WDM case, the reach in the experiment as a fraction of the simulation reach for span lengths of 111 and 136 km. The reason is the smaller number of loop round trips. For a span length of 136 km, 85-90% of the simulation reach is achieved for both PS- and PM-QPSK. The remaining gap is explained by the 0.5-0.6 dB higher implementation penalty in the experiment compared to the simulations.

## 6. Conclusion

We have performed an experimental comparison of PS-QPSK at 20 Gbaud with PM-QPSK at the same symbol rate and the same bit rate by using a recirculating loop with three different span lengths. Both a single channel system and a WDM system with nine 50 GHz-spaced channels were investigated. For the WDM case and at a BER of  $10^{-3}$  in the receiver, more than 41% and 21% increase in transmission reach was found for all span lengths when comparing the formats at the same symbol rate and at the same bit rate, respectively.

We compared our experimental findings with numerical simulations in which we used the same data rates as in the experiment. The simulation results showed slightly larger differences between the formats in favor of PS-QPSK, but good overall agreement with the experiment, especially for the longer span lengths. This is most likely due to the lesser impact from gain ripple of the loop filter and PDL when the number of circulations in the loop is smaller.

In both the experiment and the numerical simulations, the relative difference in performance of the two modulation formats was similar for the three investigated span lengths. Even with substantial span-losses of 22.5 dB (for 111 km span length) and 27.9 dB (for 136 km), 20 Gbaud PS-QPSK could in the WDM system experiment be transmitted over more than 5000 and 3300 km respectively and still achieve a BER of less than  $10^{-3}$  in the receiver. For PM-QPSK, the corresponding numbers were 3900 km and 2400 km for the same bit rate (60 Gbit/s) as PS-QPSK. These values may be increased by using fiber with lower

attenuation and/or amplifiers with smaller noise figures and show that long-haul transmission is feasible even when using standard fiber and very long span lengths.

In the simulations we also made the first comparison of the formats with differential coding of the data, and showed that PS-QPSK has a further reduction in required OSNR of 0.3 dB at a BER of  $10^{-3}$  compared to PM-QPSK at the same bit rate, resulting in further relative improvements in transmission reach.

### **Acknowledgments**

We would like to acknowledge the financial support from the Swedish Foundation for Strategic Research.